Heat-Sealed Processes in Chañar Brea Gum Films

María Fernanda Torres * , Federico Becerra , Mauricio Filippa , Gisela Melo , Martin Masuelli *

Posted Date: 17 June 2025

doi: 10.20944/preprints202506.1402.v1

Keywords: chañar brea gum; heat-sealed; films

 doi:10.20944/preprints202506.1402.v1

Article

Heat-Sealed Processes in Chañar Brea Gum Films

María Fernanda Torres [1,*], Federico Becerra [1], Mauricio Filippa [2], Gisela Melo [3] and Martin Masuelli [1,*]

[1] Instituto de Física Aplicada (INFAP-CONICET-UNSL)-Departamento de Química, Facultad de Química, Bioquímica y Farmacia, Universidad Nacional de San Luis, Ejército de los Andes 950, San Luis ZC 5700, Argentina

[2] Departamento de Farmacia, Facultad de Química, Bioquímica y Farmacia, Universidad Nacional de San Luis, Ejército de los Andes 950, San Luis ZC 5700, Argentina

[3] Facultad de Química, Bioquímica y Farmacia, IMIBIO-CONICET, Universidad Nacional de San Luis, Chacabuco 917, San Luis ZC 5700, Argentina

* Correspondence: fpeder21@gmail.com (M.F.T.); masuelli@unsl.edu.ar (M.M.)

Abstract: This work presents a comprehensive evaluation of the heat-sealability of films developed from chañar brea gum (CBG), a biopolymer with potential for packaging applications. Heat-sealability is a critical property in the packaging industry, as it directly determines the integrity and functionality of the final product. The films were prepared by the 10% casting method with the addition of glycerin and heat sealing was carried out at 140 °C using a heat sealer. The study employs a joint determination that explore fundamental properties of the films, including proximate analysis, antioxidant capacity, FTIR, DSC, TGA-DTGA, XRD, mechanical testing, water vapor permeability and sorption, and biodegradability. By integrating the results of all these determinations, the study seeks to evaluate and explain the "intimate relationships"—i.e., the complex interconnections among the molecular structure, composition, thermal behavior, mechanical properties, and barrier properties of chañar gum films—and how these fundamental properties dictate and control their heat-sealability. Thermal stability is up to 200°C with a melting point of 152.48°C for CBG. The interstrand spacing is very similar at 4.88nm for CBG and 4.66nm for CBG-H. SEM images of the heat seal show rounded shapes on the surface, while in the cross section it is homogeneous and almost without gaps. The WVP decreases from 1.7 to 0.37 for CBG and CBG-H, respectively. The Young's modulus decreases from 132MP for CBG to 96.5MPa for CBG-H. The heat sealability is 656N/m with a biodegradability of 4 days. This comprehensive approach is crucial for optimizing the sealing process and designing functional and efficient biodegradable packaging.

Keywords: chañar brea gum; heat-sealed; films

1. Introduction

One of the fundamental criteria for polymer or biopolymer films is heat sealing, primarily due to its application in the successful closure of flexible materials. In the heat sealing process, two layers of thin films are pressed between two heated metal bar jaws for a sufficient period of time, followed by cooling. The polymer melts due to this applied heat, and simultaneous interfacial interaction occurs through mass diffusion through the molten layers. Upon cooling, a rigid bond develops due to interdiffusion and entanglement of the polymers of both molten layers at the interface. Seal strength defines the maximum force per unit seal width required to progressively separate one flexible material from another flexible material, according to the ASTM F88-09 standard method (ASTM, 2009). Seal strength is measured to indicate the quality of the seal. Seal strength depends on the sealing temperature, the applied pressure, and the dwell time, i.e., the time the material remains in the heating zone. In seal strength testing, it is important to understand the failure mode of a heat-sealed material to consider the performance of the packaging and how the sealed surface separates during the seal failure assessment. The different seal failure modes are: delamination, peeling, and tearing [1,2].

 doi:10.20944/preprints202506.1402.v1

Global interest in edible and biodegradable flexible films stems from the need to reduce pollution from non-recyclable synthetic plastic packaging. These films, particularly those made from starch, show promise for packaging dry ingredients, preserving their quality, and can function as ingredient delivery systems in food processing [3,4].

For use in bags and sachets, effective heat sealing is critical. Seal strength is key to withstand handling and storage. Although heat sealing has been investigated in biodegradable films with blends of starch and other polymers (including synthetic ones), information on fully edible films is limited. Sealing properties have been studied in whey protein and zein films, with zein being found to improve heat sealing. Blends of carbohydrates and proteins have also been evaluated, with measured seal strengths [5].

However, there are few specific reports on edible films based primarily on starch. Although heat-sealed banana flour films have been used for food packaging, seal strength is not always detailed. To address this gap, recent research seeks to thoroughly evaluate the heat-sealing properties of edible films made from corn starch and functional polysaccharides, adding the latter to improve mechanical and barrier properties and achieve effective heat sealing for packaging applications [1].

Research into bio-based polymers and composites is crucial for creating sustainable alternatives to petroleum-based plastics and reducing environmental pollution [6].

The research demonstrates significant economic potential for producing biodegradable packaging from plants as an alternative to plastic pollution, although large-scale implementation still faces challenges [7].

The heat sealing property of self-supporting edible films composed of corn starch and functional polysaccharides (amylose, methylcellulose and hydroxypropylmethylcellulose), heat sealed between 85 and 166 °C, was evaluated in reference [1].

Protein films are alternatives to conventional plastics, but their mechanical and barrier properties require improvement through physical, chemical, or biochemical treatments. Although results vary depending on the method and composition, it is concluded that combining nanotechnology with enzymatic and physical treatments is the most promising way to create optimal protein packaging for various food applications [8].

Biodegradable corn/wheat starch films were developed with lemon essential oil (LEO) and surfactants. The addition of LEO and surfactants modified their physical properties and significantly increased their antimicrobial activity. These films have potential as biodegradable active packaging to control microbial food spoilage [9].

To improve the properties of edible soluble soy polysaccharide (SSPS) films with gelatin addition, creating blended films with improved heat sealability, strength, and stability. These SSPS/gelatin blended films are promising candidates for rapidly dissolving packaging of powdered products [10].

A biodegradable bag for fish and meat was developed using cellulose acetate and cellulose nanofibers. Natural anthocyanin was incorporated to create an ammonia sensor that indicates freshness through color change. This heat-sealable film has good properties and potential as an active biodegradable packaging with a freshness indicator [11].

Biodegradable active films of starch-chitosan reinforced with reduced graphene oxide were developed that improved functional properties and maintained heat sealability for food packaging [12].

The effect of the glycerol/sorbitol ratio on the properties, including heat sealing, of cassava starch films was studied. A 1:1 ratio of glycerol and sorbitol resulted in the best strength and sealing morphology, highlighting the need to optimize the combination of plasticizers [13].

Heat sealing is key to sealing flexible packaging, forming bonds through diffusion and crosslinking of polymers upon heating. Seal performance (strength and tightness) is vital to food safety and quality, influenced by material properties and sealing parameters. Optimizing the selection of thermoplastic materials by understanding their thermal transitions is crucial to achieving seals with the strength and tightness required for flexible packaging [14].

 doi:10.20944/preprints202506.1402.v1

Biodegradable films were developed from soy protein isolate (SPI) with Tara pod extract (TPE) for packaging. The addition of TPE improved mechanical properties, UV/oxygen barrier properties, and heat sealing. These TPE-SPI films showed potential for packaging fatty foods, offering greater protection than polyethylene containers [15].

Starch-based packaging is a sustainable and affordable alternative for reducing plastic pollution in developing countries with limited recycling infrastructure. Although laboratory-level formulation is advanced, there are significant practical challenges along the value chain, including industrial processing, storage, and moisture resistance. Comprehensively addressing these stages is crucial for scaling up production and achieving successful implementation to replace single-use plastics [16].

Active, printable, and heat-sealable HPMC/cellulose nanofiber films with propolis-loaded zein nanoparticles were developed, showing potential as an environmentally friendly alternative to plastic for food packaging [4].

"Greek salad"-style edible films were created from vegetable purees and pectin, with and without olive oil/guar gum, and characterized. All films showed good heat-sealing properties, but the additions offered no significant advantages. The focus in the future is on optimizing the basic film for packaging fatty foods [17].

Enhanced pectin-active films were developed with curcumin-loaded phytoglycogen nanoparticles, achieving improved barrier, antioxidant, and antibacterial properties, with the potential to replace heat-sealable plastics in oil packaging [18].

Chitosan is a promising antimicrobial biopolymer for biodegradable packaging that extends food shelf life. Further research is needed to optimize its properties and commercialization [19].

Given the limitations of conventional sealing techniques for biopolymers, a novel, nontoxic and sustainable adhesive based on rice biopolymer, chitosan, and alginate was developed. This formulation proved effective in bonding biopolymer surfaces with good strength, even under high humidity conditions. It represents a promising and safe alternative for sealing bio-based films and materials [20].

Heat-sealable soy protein films reinforced with cow horn were developed, proving to be smart (pH-sensitive) and environmentally friendly packaging with good mechanical properties and UV protection for food [21].

For example, the authors of references [22,23] highlight heat sealing as a key packaging technique for ensuring the integrity of polymeric containers, achieved by fusing and bonding films using heat and pressure. Seal strength is a measure of seal quality, assessed in tensile tests that identify failure modes according to ASTM F 88-00.

Chañar brea gum (CBG), extracted and purified from *Parkinsonia praecox*, is a water-soluble hydrocolloid (solubility increases with temperature). Its solutions increase in viscosity with increasing CBG concentration and decreasing temperature, and pH also affects the viscosity [24]. The density of the solution at 25°C increases linearly with concentration until saturation. GB reduces the surface tension of water at 5% concentration. CBG is useful as a stabilizer/emulsifier, foam former, and film former.

This study focused on the formulation of CBG-based films and coatings with glycerol used as a plasticizer [25]. The CBG films displayed amber-colored transparency, with a dense and homogeneous structure at the microscopic level. Wetting capacity increased with the addition of glycerol, while the water solubility of the films increased with temperature. Water vapor permeability remained stable up to 20% glycerol, increasing thereafter. Glycerol also reduced opacity and tensile strength [25].

This study investigated how to improve the functional properties of CBG films by adding montmorillonite (MMT). The incorporation of MMT into the film-forming GB solution reduced foaming. The resulting films, created by casting MMT exfoliated within the CBG matrix, showed that their optical properties depended on the nanofiller concentration. The addition of MMT decreased the films' solubility, moisture uptake, and water and gas permeability. Furthermore, an increase in Young's modulus and tensile strength was observed, albeit with a reduction in elongation [26].

 doi:10.20944/preprints202506.1402.v1

Water transport in edible films made of hydrophilic polymers is complex. This study thermodynamically and phenomenologically analyzed the incorporation of montmorillonite (Mt) nanoparticles into CBG films. Moisture adsorption isotherms showed that the presence of Mt makes the exothermic adsorption process less favorable, reducing water uptake. Changes in entropy and isosteric heat suggest a more stable and ordered structure in films containing Mt. The Gibbs energy indicated a lower affinity for water in the composite films. Water vapor permeability in CBG films decreases with the addition of Mt, due to the increased tortuosity created by the nanoparticles and the decreased hydrophilic character of the matrix [27].

In reference [28], edible films of whey protein concentrate (WPC) were prepared with lipids (sunflower oil or beeswax) to improve their water vapor barrier, using CBG as an emulsifier and matrix component. Ultrasonication was used to obtain homogeneous emulsions with small droplet sizes. CBG helped to reduce the emulsion droplet size, especially at lower lipid contents. The emulsions presented negative zeta potential due to the pH and isoelectric point of CBG and proteins. The increase in lipids in the films reduced the mechanical strength, being better the films without lipids. The addition of lipids decreased the water vapor permeability (WVP), an effect that was enhanced by CBG. Films with CBG presented a slight amber color. Overall, GB proved to be a good emulsifier for the lipid fraction and improved the homogeneity and mechanical properties of the WPC-lipid composite films.

In this study, given in reference [29], bilayer films were formulated using pectin and CBG, comparing their functional properties with those of single-layer films of each component. Microscopic and surface observations confirmed the integrity of the bilayer films, with no delamination. The high solubility of the CBG films also influenced the solubility of the bilayer films. The water vapor permeability of the bilayer films depended on the layer exposed during desorption, being lower than that of CBG films alone, but higher than that of pectin films of similar thicknesses. The distinct properties of each layer in the bilayer films make them potentially interesting for applications such as controlled drug release.

This paper presents a comprehensive evaluation of the heat-sealing capability of films developed from chañar gum (pitch gum), a biopolymer with potential for packaging applications. Heat-sealability is a critical property in the packaging industry, as it directly determines the integrity and functionality of the final package, ensuring the protection of the product inside. The heat-sealing process involves the controlled fusion of the surfaces of two films through the application of heat and pressure, followed by cooling that solidifies the bond. To fully understand this heat-sealing behavior and its underlying mechanisms, the study employs a battery of determinations that explore fundamental properties of the films: proximate analysis, antioxidant capacity, FTIR, DSC, TGA-DTGA, XRD, mechanical testing, water vapor permeability and sorption, and biodegradability. By integrating the results obtained from all these determinations, the study seeks to evaluate and explain the "intimate relationships"—that is, the complex interconnections between the molecular structure, composition, thermal behavior, mechanical properties, and barrier properties of chañar gum pitch films—and how these fundamental properties dictate and control their heat-sealability. This comprehensive approach is crucial for optimizing the sealing process and designing functional and efficient biodegradable packaging.

2. Materials and Methods

2.1. Raw Material

Chañar brea gum was collected by the “Viva el Monte” from the exudate of the *Parkinsonia praecox* tree located in 32°06'36.5"S, 65°03'56.8"W named “La Travesía”, Traslasierra, Córdoba, Argentina.

The procedure consists of dissolving the exudate in distilled water and then filtering it. This filtrate is precipitated with ethanol in a 70/30 ratio in distilled water. It is filtered again, and the retentate is dried at 60 °C for 24 hours [30–32].

 doi:10.20944/preprints202506.1402.v1

The yield was calculated from 100 g CBG, using the following equation:

$$Yield\% = 100\frac{CBG_{sol}}{CBG} \quad (1)$$

where CBG was the initial mass (100 g) and CBG_{sol} was the mass of resulting filtration processes [33].

2.1.1. Film Preparation

The films preparation was carried out by adding 10 g CBG in 100mL water and 5 mL of glycerin used as plasticizer and molded in box of 29cm x 21cm x 4cm. Next was dry at 60°C by 24hs. Finally, it was unmolded and packaged in a self-sealing polyethylene bag [25,27].

2.1.2. Film Heat-Sealing

Heat-sealing was performed on an OX400 bag sealer (Oryx, China) at 140°C, 3 mm wide, for 3 seconds. The samples to be heat sealed were cut into rectangular strips of film, each 100 mm long and 20 mm wide. The strips were conditioned at 40% (RH) and a temperature of 25°C for 24 hours. For sealing, two conditioned strips were placed one on top of the other and sealed. Heat sealing is studied in a conventional way, that is, horizontal heat sealing (CBG-H), and vertical heat sealing (CBG-V) was evaluated. Measurements were repeated 3 times. Seal strength was determined according to the ASTM F88-09 method (ASTM, 2009) using a Brookfield CT3 texturometer (U.S.A.). The maximum force (N) required to peel/tear the seal was recorded numerically and graphically, and the failure mode was simultaneously noted. Seal strength was calculated as the maximum force/film width [1].

2.1.3. Proximate Analysis of Biomass

Proximate analysis of the macerated biomass powder was performed according to AOAC standard methods (AOAC, 2012). Nitrogen content was measured via the Kjeldahl–Arnold–Gunning method, calculating total proteins with a 6.25 factor (AOAC. 920.12); protein productivity (mg/L/hour) was also determined. Total fats were analyzed by the Soxhlet gravimetric method using petroleum ether (Sigma Aldrich) (AOAC 945.39). Crude fiber analysis used the digesting sample method with H_2SO_4 and NaOH (Sigma Aldrich) (AOAC 962.09). Ash content was found by weight difference after calcining the sample (AOAC 945.46), and moisture content by heating under reduced pressure (AOAC 945.46). Carbohydrates were calculated indirectly: Total carbohydrates=100−(Proteins+Total Fat+Moisture+Ash). Following these standard procedures ensured accurate and consistent results, providing valuable data for research and industry [34].

2.1.4. Antioxidant Activity Assays

Reactive oxygen species (ROS), such as superoxide anion radicals (O^{*2-}) and DPPH radicals, are recognized culprits behind oxidative damage and functional decline, notably affecting the liver. Given the detrimental impact of ROS, investigating novel polysaccharides as potential countermeasures is vital for developing effective treatments for liver damage and oxidative stress-related conditions. Consequently, the determination (or measurement) of these harmful free radicals is a crucial prerequisite in evaluating such polysaccharides and uncovering their therapeutic potential. Research in this area, by studying the interaction between novel polysaccharides and ROS, holds promise for leading to significant breakthroughs in healthcare and wellness [35].

Reducing Power

Based on the method described in reference [35], a reducing power assay was conducted to determine the reducing capacity of polysaccharide solutions. Executing this method required precision and careful incubation. The procedure involved adding phosphate buffer (2 M, pH 6.6), potassium ferricyanide (1% wt.), and trichloroacetic acid (10% wt., 2.5 mL) to halt the reaction. Subsequently, ferric chloride (0.2 mL) was introduced, and the absorbance at 700 nm was recorded. For ensured reliability, the assay was conducted in triplicate, incorporating gallic acid as a positive

 doi:10.20944/preprints202506.1402.v1

control. The outcomes were presented as meq/mL of gallic acid, reflecting a rigorous approach to assessing reducing power.

DPPH Scavenging Activity

To determine the DPPH radical scavenging activity of polysaccharide solutions, a method based on reference [35] with some adjustments was employed. The protocol involved combining volumes of polysaccharide solution (tested across a range, such as 0.1 to 1 mL) with a 90% ethanolic DPPH solution (0.15 M). Following a 30-minute incubation period protected from light, the absorbance was recorded at 517 nm. Total antioxidant content was quantified as a percentage of antioxidant activity (% AA) through the application of the provided equation:

$$AA(\%) = \frac{(Ac-(Am-Ab))}{Ac} \times 100 \quad (2)$$

Following absorbance measurements, calculations utilized a formula incorporating the absorbance of the control (A_c), the sample absorbance (A_m), and the blank absorbance (A_b). The entire procedure was executed in triplicate to ensure robust reliability. Ascorbic acid served as the positive control; a calibration curve was constructed based on measurements from ascorbic acid standards. This calibration curve allowed results to be expressed as mg/mL equivalents of ascorbic acid. Such diligent measurements and subsequent computations yielded valuable insights into the antioxidant properties and potential health benefits of the polysaccharides [35].

Total Polyphenol Content

Total phenolic compounds were determined employing the Folin–Ciocalteu method [35–37], adapted with modifications to enhance accuracy and precision. The protocol involved carefully combining a 5 mL sample aliquot with 1.5 mL of Folin–Ciocalteu reagent (2 N) and 15 mL of 15% Na_2CO_3 solution in a volumetric flask. The volume was then adjusted to 25 mL with distilled water. The resulting solution was incubated for 2 hours at room temperature, protected from light, to allow the reaction to complete. Absorbance was subsequently measured at 760 nm. For quantification, a calibration curve was established using gallic acid (GA) as a reference standard, with six concentrations ranging from 1 to 6 mg/L being prepared and measured. To confirm the reproducibility and reliability of the data, the entire analytical procedure was meticulously repeated.

2.2. Fourier-Transform Infrared Spectroscopy

In this study, Fourier transform infrared spectroscopy (FTIR), a common technique in analytical chemistry for identifying chemical compounds, was employed. Spectra were obtained using a Nicolet PROTEGE 460 spectrometer in two modes: diffuse reflectance (DRIFTS) and transmission. Data collection was performed in the 700–400 cm^{-1} range, scanning each sample 64 times to ensure accurate results. The combined use of both modes allowed for a detailed analysis of the samples' chemical composition, structure, and molecular vibrations, ensuring the robustness and reliability of the obtained spectra for meaningful interpretation [38].

2.3. X-Ray Diffraction (XRD)

X-ray diffraction (XRD) studies were carried out using an advanced Rigaku ULTIMA IV type II instrument (Tokyo, Japan). This instrument employed a Cu Kα lamp with a wavelength (λ_B) of 1.54 Å and a nickel filter for accurate measurements. Scanning was performed in the 2θ range from 3° to 60°, operating the equipment at 30 kV and 20 mA. Data collection was carried out continuously at a speed of 3° per minute and a reading step of 0.02°. The average interlaminar distance ($d_{spacing}$) was calculated using the Bragg equation.

 doi:10.20944/preprints202506.1402.v1

$$d_{spacing} = \frac{n\,\lambda_B}{2sin\theta_B} \quad (3)$$

where $d_{spacing}$ represents the intercatenary distance, θ_B refers to Bragg's angle, n is an integer value determined through analysis, and λ_B denotes the X-ray wavelength used [49].

$$I_{cr} = 100\ \frac{I_{max} - I_{ad}}{I_{max}} \quad (4)$$

In addition, the crystallinity index (I_{Cr}) was calculated from the normalized diffractogram. For this purpose, the intensities of the peaks corresponding to the lattice planes were used, such as the (110) reflection (I_{max}), observed around 21°, which represents the maximum intensity. The intensity of the amorphous diffraction (I_{ad}), taken at approximately 15°, was also used, following methodologies described in the previous literature [39,40] to determine the I_{Cr}.

2.4. Differential Scanning Calorimetric Analysis (DSC)

Differential scanning calorimetry (DSC) was performed using a STA 449F3-Jupiter (Selb, Germany). Approximately 5 mg of biopolymer sample was placed in an alumina crucible and heated from 25 °C to 400 °C at a constant rate of 5 °C per minute. This process was carried out under a dynamic nitrogen atmosphere with a flow rate of 25 mL/min, parameters selected to accurately analyze the thermal behavior, characteristic transitions, and stability of the biopolymer [41].

2.5. Thermogravimetric Analysis

The thermal stability of the polysaccharide films was determined by thermogravimetric analysis (TGA) using a TA Instruments TG 295 analyzer. Samples of approximately 8 mg were heated at 10 °C/min under a pre-filtered N2 (99.99%) atmosphere with a flow rate of 50 mL/min, using empty aluminum crucibles as reference. Temperature calibration was performed with indium (melting point 156.60 °C) and the Curie point of Ni (353 °C) [42].

2.6. Scanning Electron Microscopy (SEM)

The film morphology was meticulously analyzed using a LEO 145VP scanning electron microscope (SEM), complemented by energy dispersive X-ray (EDAX) analysis using an EDS Genesis 200. For SEM observation, samples were prepared by immersion in liquid nitrogen and gold coating. Analyses were performed under high vacuum, with EDAX spectra obtained at an accelerating voltage of 120 kV to ensure accurate data collection of elemental composition [43].

2.7. Mechanical Tests

The mechanical properties of the materials were evaluated using a Brookfield CT3 instrument, in accordance with ASTM D882. Tests were performed in triplicate at 25 °C and 40% relative humidity, with a constant tensile rate of 0.1 mm/min. Samples of 40 mm length by 10 mm width were used, and the thickness of each film was measured with a micrometer. Force (F) and strain (Δl) data were recorded until failure. Tensile strength (σ) was calculated as the maximum load divided by the initial cross-sectional area (A), percentage elongation at break (% ε) as the percentage change from the initial length (l=40 mm) at failure, and elastic modulus (E) as the slope of the stress (σ) vs. strain (ε) curve in the linear elastic region. [43,44].

$$E = \frac{\sigma}{\varepsilon} \quad (5)$$

$$\sigma = \frac{F}{A} \quad (6)$$

$$\varepsilon = \frac{\Delta l}{l_0} \quad (7)$$

 doi:10.20944/preprints202506.1402.v1

2.8. Water Vapor Permeability

Water permeability was determined using Electrotech Systems equipment that controlled temperature and humidity in a closed system. Weight change was recorded using a RADWAG balance accurate to 0.1 mg, and film thickness was measured using a Kolfe micrometer accurate to 0.1 mg. Circular film samples, 25 mm in diameter, of measured thickness were placed in the perforated caps of bottles containing 20 g of silica gel. The sealed bottles were maintained at 30 °C and 85% relative humidity, and weight changes were recorded according to a detailed schedule for 24 hours, following ASTM E96.

$$\tau = \frac{Q}{t\,A} \tag{8}$$

$$P = \frac{\lambda}{\Delta P}\,\tau \tag{9}$$

where τ is transmission speed (ng/m²s), ΔP is pure water vapor pressure (4238.605 Pa), t is measurement time(s), Q is permeating mass (ng), λ is thickness of film (m) and A is area of cell (m²) [43–45].

Biodegradability

Biodegradation is the breakdown of biopolymers by microbial enzymes (bacteria, yeast, fungi), which can be total (generating methane or CO_2) or partial (changing composition/properties). A recent study evaluated biodegradation rates in a container covered with moistened soil (85% RH, 30 °C) for 30 days. These findings improve the understanding of biodegradation mechanisms and their implications for sustainable waste management [43,44].

3. Results

3.1. Proximate Analysis of Biomass and Antioxidant Capacity

Starting with 100 grams of chañar brea exudate, an extraction process was carried out to obtain purified chañar brea gum (CBG), achieving a highly efficient extraction. The specific yield achieved in the operation was 82.33±2.45%. This means that the vast majority of the initial exudate could be converted into gum. This yield underscores the effectiveness of the extraction method employed. The analyzed product exhibits notable antioxidant and bioactive properties, evidenced by a DPPH value of 9.81±0.32 meq/L ascorbic acid equivalent. Its polyphenol content is 1.16±0.034 meq/g of gallic acid, quantified using the Folin–Ciocalteu method. In addition, it demonstrates a hydroxyl radical (OH*) scavenging capacity of 4.2±0.25% and a reducing power of 4.89±41 meq/g, which underscores its potential activity. Regarding its nutritional composition, it is distinguished by being predominantly a source of total carbohydrates, constituting 86.97±3.77% of its weight. It provides a moderate protein content (6.36±023%) and is significantly low in total fat, representing only 1.19±0.03%. Other components analyzed include 4.07±0.15% ash, 3.12±0.11% moisture, and an extremely low sodium content of just 0.0114±0.002%. Similar results can be found for pectin and *Lithraea molleoides* gum and chañar gum (*Geoffrea decorticans*) [33,44]. No changes were recorded in proximal analysis and antioxidant capacity of heat-sealed CBG films.

3.2. X-Ray Diffraction (XRD)

Data obtained through techniques such as X-ray diffraction (XRD) are essential for characterizing these polysaccharides, even though they are predominantly amorphous. These data, particularly d-spacing, allow us to infer crucial information about the intermolecular distances between polymer chains, as well as to identify structural modifications induced by environmental changes such as moisture content or temperature fluctuations. Understanding this structure at the molecular level is vital for the development of new materials with improved functionalities. In the

 doi:10.20944/preprints202506.1402.v1

context of the packaging industry, modulating these structures can translate into the creation of films with superior barrier properties against gases such as oxygen, thus significantly extending the shelf life of the food products that come into contact with them [46].

Amorphous polysaccharides are a fundamental component of numerous natural and synthetic materials. Therefore, a thorough understanding of their structural properties is essential in fields as diverse as pharmaceuticals, food science, and materials engineering. A key analytical technique for this purpose is X-ray diffraction (XRD). Although amorphous polysaccharides do not exhibit the sharp peaks characteristic of crystalline materials, their XRD patterns provide valuable information about the arrangement and organization of their molecular chains. Analysis of these diffuse patterns, including their numerical characteristics, serves as a basis for describing the structure and properties of these polysaccharides. Comparing these diffraction patterns with standard references or known structures of related compounds or polymers provides important details about their arrangement at the atomic and molecular levels, even in the absence of long-range crystalline ordering [46].

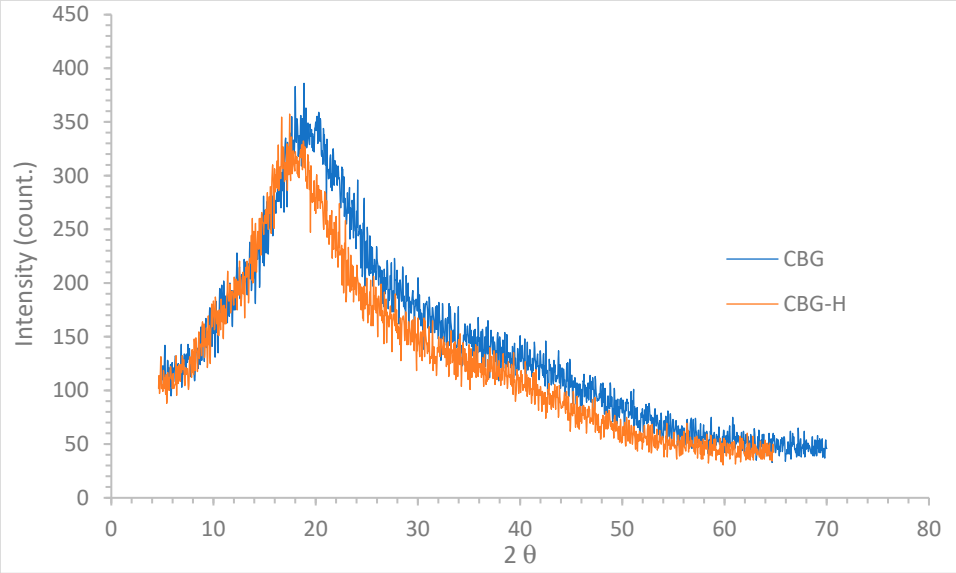

Figure 1. XRD of gums.

Table 3. XRD data of gums.

Flour	2θ	$d_{spacing}$ (nm)	I_{Cr} %
CBG	18.15 ± 0.72	4.88 ± 0.97	34.16 ± 0.97
CBG-H	19.05 ± 0.84	4.66 ± 0.91	32.54 ± 0.89

The X-ray diffraction (XRD) results for the CBG film revealed significant differences in its molecular structure after heat sealing. Initially, the unheat-sealed film showed a d-spacing value of 4.88 nm and a crystallinity index of 34.16%. D-spacing, which represents the distance between atomic or molecular planes within the material's crystalline structure, suggests a certain level of organization of the polymer chains. The crystallinity index, on the other hand, indicates the percentage of the material that exhibits an ordered, crystalline structure compared to the amorphous and disordered fraction [47]. No changes were recorded in DRX of heat-sealed CBG-H and CBG-V films.

After applying the heat sealing process of CBG-H, the XRD results showed a decrease in both parameters. The d-spacing was reduced to 4.66 nm and the crystallinity index decreased to 32.54%. This shrinkage in d-spacing could be interpreted as a rearrangement of the polymer chains to a slightly smaller interlayer distance, possibly induced by the thermal energy applied during heat sealing. The decrease in the crystallinity index suggests that the heat treatment caused a slight loss of the ordered structure in favor of a more amorphous phase [48].

This reduction in crystallinity after heat sealing is not a universal phenomenon in all polymers, as it depends on the specific nature of the material and the process conditions. However, in some

 doi:10.20944/preprints202506.1402.v1

cases, partial melting or thermal stress during heat sealing can alter existing crystalline regions or hinder the formation of new ordered structures during cooling, leading to a net decrease in crystallinity. These changes in the nanostructure of the CBG film, evidenced by the variation in d-spacing and crystallinity index determined by XRD, are crucial to understand how heat sealing affects the physical and mechanical properties of the material, such as its barrier, flexibility or sealing strength [49].

A chitosan film presented two distinctive peaks at 10.46° and 20.1° (2θ), typical of its semi-crystalline nature [50]. Carboxymethylcellulose (CMC) [50] exhibited a characteristic peak at 20.71° (2θ), reflecting its structure with a degree of ordering, although probably lower than native cellulose due to substitution. Materials designated CBG and CBG-H, showed peaks at 18.15° and 19.05° (2θ), suggesting the presence of specific crystalline structures of these materials. In contrast, the study of sonicated spores of *Ganoderma lucidum* [51] revealed a significant impact of physical treatment. These spores lost their original chitosan morphology, experienced a dramatic decrease in their degree of crystallinity (shifting toward a more amorphous state), and showed an increase in the degree of deacetylation of their constituent chitosan. Taken together, the XRD results demonstrate how the technique allows for the identification of crystalline structural features of different polymers and biological materials, which can contribute to the disruption of crystallinity [48].

3.3. Fourier-Transform Infrared Spectroscopy (FTIR)

Analysis of the infrared spectrum (Figure 2) identifies prominent absorption bands linked to specific functional groups. Hydroxyl groups are indicated by the –OH stretching band at 3430 cm^{-1}. C–H stretching occurs at 2920 cm^{-1}, and a general carbonyl band is present at 1740 cm^{-1}. More specifically, the carboxylate group shows a characteristic carbonyl band at 1640 cm^{-1} (C=O from $–COO^-$). Bending vibrations from $–CH_2OH$ side chains produce multiple bands at 1420 cm^{-1} and 1380 cm^{-1}. A strong peak at 1250 cm^{-1} is assigned to C–O–C stretching. C–O glucopyranosic bending is seen around 1040 cm^{-1}, and a signal at 890 cm^{-1} may suggest the presence of a C-N bond. Out-of-plane C–O bending vibrations are detected at 775 cm^{-1} [43,44]. Together, these assignments provide a detailed picture of the compound's structure. No changes were recorded in FTIR of heat-sealed CBG films.

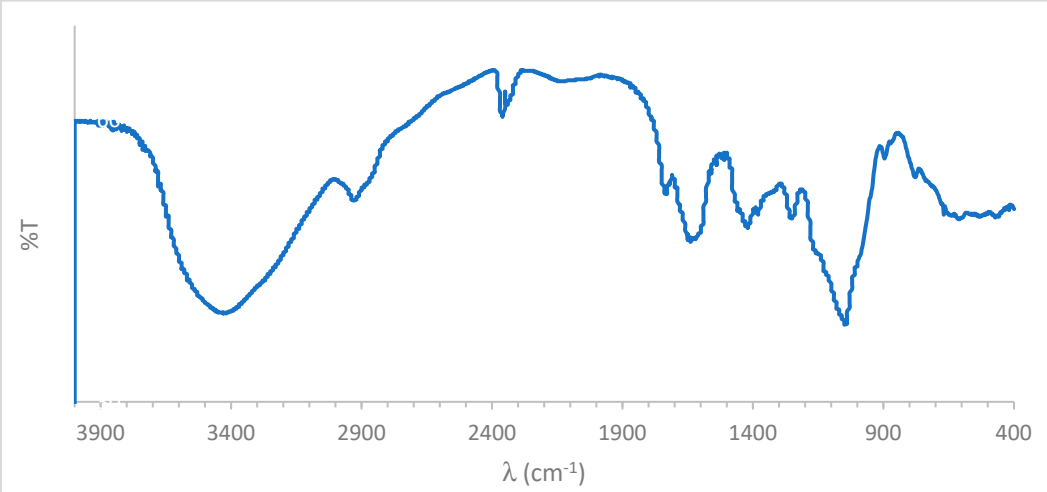

Figure 2. FTIR of CBG.

3.4. Differential Scanning Calorimetry (DSC)

Differential Scanning Calorimetry (DSC) analysis of CBG provides essential information about its thermal transformations, see Figure 3. The DSC initially reveals a clear glass transition (T_g) at 43.78 °C. This second-order transition marks the point at which the amorphous regions of CBG transition from a rigid, glassy solid state to a more flexible, rubbery state with greater molecular mobility. T_g is

 doi:10.20944/preprints202506.1402.v1

a critical parameter for predicting the behavior of amorphous materials, affecting their mechanical stability, reaction kinetics, and diffusion properties. An endothermic peak is then observed around 75.85 °C, associated with an enthalpy of 216.2 J/g. The endothermic nature of this energy-intensive event, combined with its temperature, strongly suggests the desorption or elimination of potentially adsorbed water from the sample. The presence of moisture, even in small amounts, can significantly influence the T_g and stability of CBG, making this peak relevant to understanding its behavior under different ambient humidity conditions.

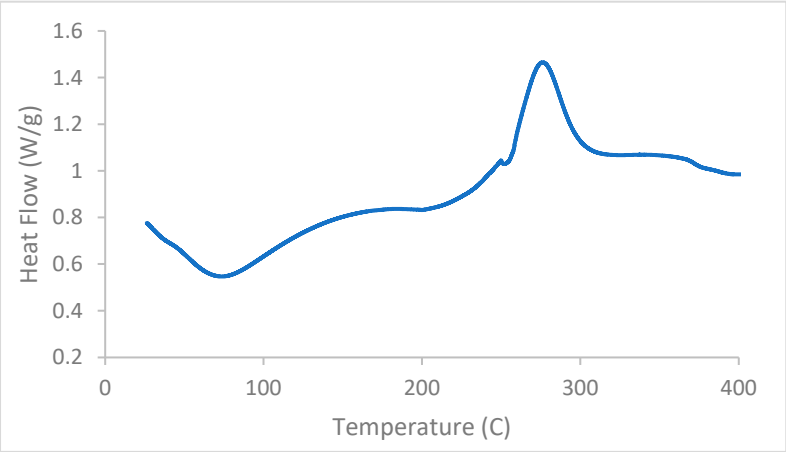

Figure 3. DSC of CBG.

Continuing to increase in temperature, the DSC displays a prominent first-order phase transition: the melting peak (T_m) at 152.48°C. This pronounced endothermic peak represents the energy absorbed during the melting of crystalline CBG, transforming it from solid to liquid. The melting temperature is an intrinsic property of a crystalline substance and a key indicator of its purity. Finally, at a higher temperature, near 275.39°C, another significant endothermic peak appears with an area of 369.9 J/g. This high-temperature thermal event, which also requires the absorption of a considerable amount of energy, is indicative of CBG degradation or thermal decomposition processes. The temperature at which this decomposition peak occurs is critical for determining the compound's thermal stability and establishing safe temperature limits for its processing and long-term storage, ensuring that the CBG maintains its chemical integrity and potency. Similar discussion for different biodegradable film materials can be found in reference [53].

3.5. Thermogravimetric Analysis (TGA-DTGA)

According to TGA and DTGA analysis of CBG, demonstrates thermal stability up to approximately 200°C. Below this temperature, both materials exhibit minimal mass loss, indicating the absence of significant degradation or evaporation of volatile components. Above 200°C, the TGA and DTGA show begin to show more pronounced mass losses, see Figure 4. This suggests that, up to this temperature limit, CBG maintains its structural integrity and composition. Therefore, 200°C represents a critical point in its thermal behavior before decomposition processes begin, where the reference [54] gives a thermal stability value less than 250°C.

 doi:10.20944/preprints202506.1402.v1

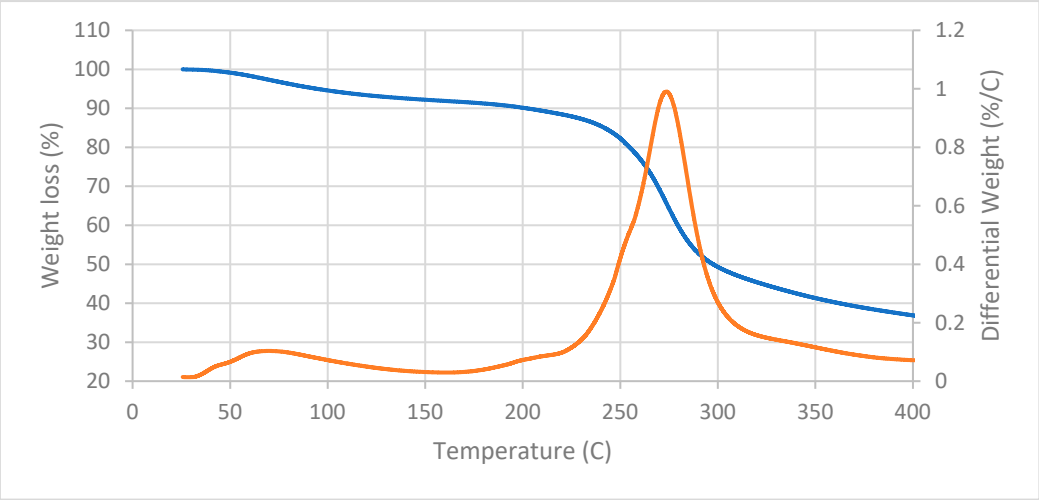

Figure 4. TGA and DTGA of CBG.

3.6. Scanning Electron Microscopy (SEM)

In Figure 5 presents a scanning electron microscopy (SEM) image of the cross-section of a heat-sealed chañar brea gum (CBG-H) film. In this micrograph, the heat-sealed area of the CBG-H film is clearly visible, appearing well-defined, allowing the area where heat was applied to seal to be visually distinguished. The heat-seal joint does not show any gaps or cracks and is almost homogeneous.

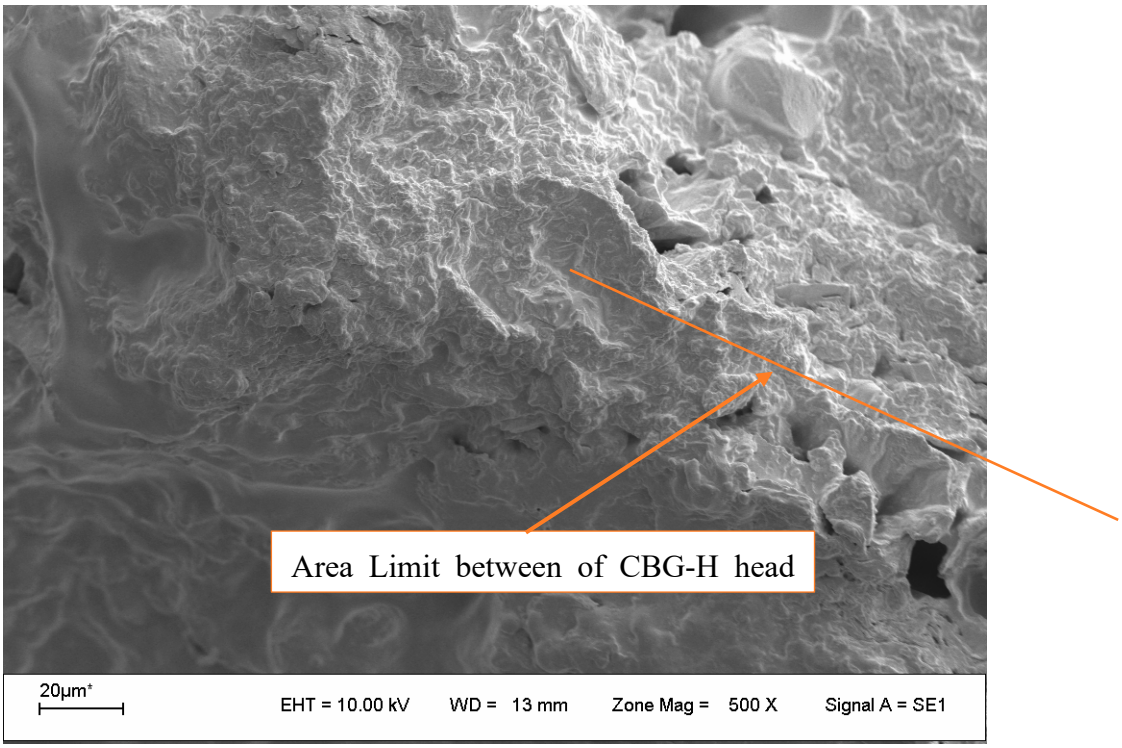

Figure 5. Cross section of CBG-H film.

The surface image of the heat-sealed film offers a detailed view of its surface morphology (see Figure 6a). A general gray background, characteristic of the base material, can be seen. Against this relatively uniform background, certain shadows with a more rounded morphology stand out. These shadows appear as alterations in the film's surface texture or topography in the heat-sealed area. For clear identification and visual reference, these specific areas, which correspond to the section where heat was applied to perform the seal, have been indicated by arrows. The appearance of these rounded shadows, unmistakably indicated by the arrows on the gray background of the film,

 doi:10.20944/preprints202506.1402.v1

precisely and clearly delimits and shows the specific section that was subjected to the heat-sealing process, allowing it to be differentiated from the rest of the film's surface (see Figure 6b).

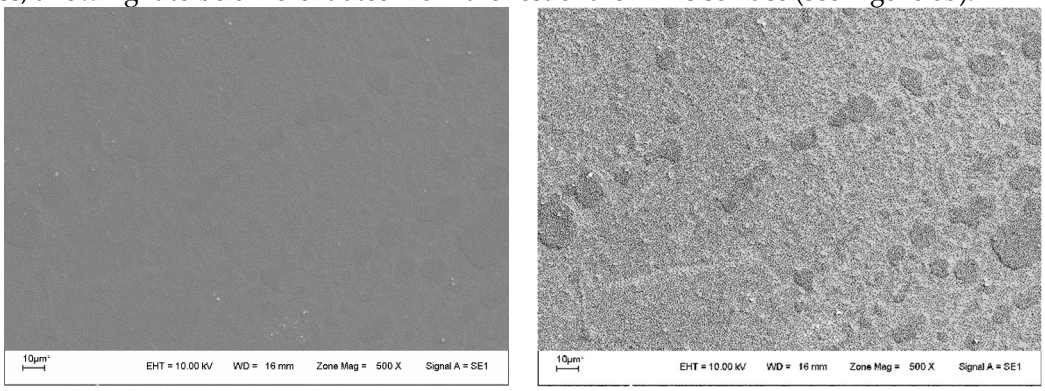

(**a**) (**b**)

Figure 6. a- Surface SEM image of heat sealing CBG-H film. b- 90% de contrast.

According to the analysis of images obtained by scanning electron microscopy (SEM), both in cross-section and in surface view (Figure 7a), the chañar brea gum (CBG) film that has not been heat-sealed exhibits distinctive structural characteristics, similar to reference [25,55]. The cross-sectional image allows an in-depth observation of the internal organization of the material (Figure 7b). In this view, the absence of large pores, significant cavities, or noticeable internal separations suggests a compact and dense structure. At the same time, the surface image provides information on the texture and uniformity of the film's outer layer. In both perspectives, homogeneity is evident; the micrograph presents a uniform appearance along its length, without showing clearly separated distinct phases, irregular accumulations of material, or abrupt variations in density or surface texture. This dense and homogeneous structure observed both on the surface and inside the non-heat-sealed CBG film indicates a uniform distribution of its components and a robust internal cohesion before any localized heat treatment such as heat sealing.

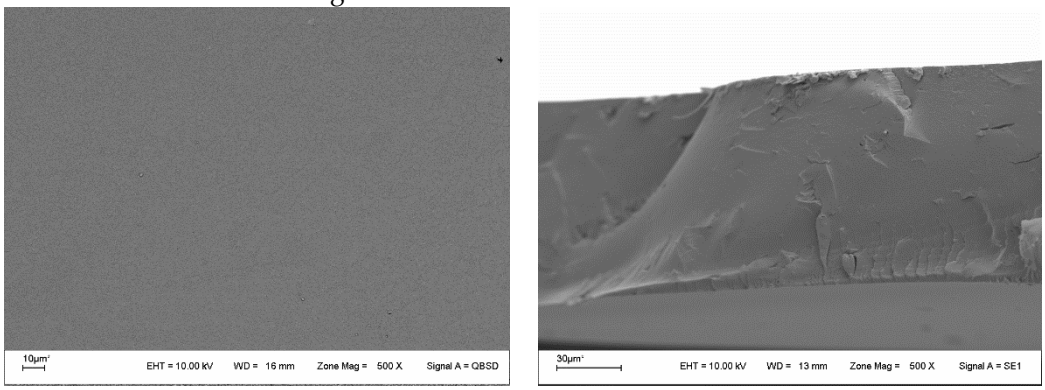

(**a**) (**b**)

Figure 7. a- Surface image of CBG film without heat sealing. b- Transversal cut.

3.7. Water Sorption and Water Vapor Permeability

Comparison of the water vapor interaction properties of standard chañar brea gum (CBG) and horizontally heat-sealed chañar gum (CBG-H) reveals notable differences. The standard CBG sample exhibits a water vapor sorption rate of 3.40 g/g, indicating a high capacity to absorb moisture from the environment. In contrast, horizontally heat-sealed chañar brea gum (CBG-H) shows a significantly lower sorption rate of only 1.16 g/g. This difference suggests that the heat-sealing process drastically reduces the material's affinity for water.

Similarly, water vapor permeability differs substantially. The standard CBG exhibits a permeability of 1.70 ng m/(m² s Pa), implying that water vapor passes through the film with relative ease. On the other hand, horizontally heat-sealed CBG-H has a much lower permeability, of 0.37 ng

 doi:10.20944/preprints202506.1402.v1

m/(m² s Pa). This demonstrates that horizontal heat-sealing gives the film a much more effective barrier to water vapor penetration.

Considering these findings in conjunction with other possible effects of heat-sealing, such as a potential reduction in water sorption capacity (absorption/adsorption), these data indicate that the horizontal heat-sealing treatment significantly and quantifiably improves the moisture barrier properties of chañar brea gum film. The combination of lower sorption and such a significant reduction in water vapor permeability positions the CBG-H film as a considerably more promising and suitable material for use in various applications where actively controlling moisture transfer is crucial, such as packaging for moisture-sensitive products, protective coatings, or components in products requiring dry environments. For a more in-depth discussion, see reference [56].

3.8. Mechanical Test and Heat-Sealing Capacity

A thorough comparison of the mechanical properties of chañar pitch gum (CBG) films reveals that both the initial film thickness and the heat-sealing method employed have a considerable influence on its performance under tension. Analyzing the maximum elongation at break, a key indicator of the material's flexibility and stretchability before failure, a marked difference is observed. The CBG sample with a thickness of 190 microns exhibits a significantly lower maximum elongation of just 5.11%. This contrasts markedly with the heat-sealed samples, where the CBG-H (horizontally heat-sealed) reaches 11.09% and the CBG-V (vertically heat-sealed) reaches 12.13%. This disparity suggests that either the base film used for heat sealing is inherently more extensible, or the heat sealing process itself induces structural changes that increase the ductility of the film in the analyzed area, allowing it to deform much more before breaking compared to the standard film of lower thickness.

Table 4. Films mechanical test.

Film	e (μm)	ε_{max}%	τ_{max} (MPa)	E(MPa)
CBG	190	5.11	4.48	132.0
CBG-H	307	11.09	3.36	96.8
CBG-V	305	12.13	4.58	159

Regarding the ultimate tensile strength, which quantifies the maximum tensile force the material can withstand before fracturing, values also vary between samples. The CBG film of 190 μm has an intermediate value of 4.48 MPa. The CBG-H sample records the lowest ultimate tensile strength of the group, at 3.36 MPa with thickness of 307 μm, which could indicate some weakness induced by horizontal heat sealing. In contrast, the CBG-V proves to be the most tensile, reaching 4.58 MPa, slightly surpassing even the 305 μm sample. This suggests that vertical heat sealing, unlike horizontal, appears to maintain or even slightly improve the material's inherent resistance to tensile fracture.

Finally, examining Young's modulus, a measure of stiffness or how resistant the material is to elastic deformation under stress, clear differences are evident. The 190 μm CBG sample has a modulus of 132 MPa, placing it at an intermediate stiffness within the group. The CBG-H sample, with a modulus of 96.8 MPa, is noticeably less stiff, consistent with its greater elongation and lower tensile strength; it is a "softer" or more flexible material. In contrast, the CBG-V sample exhibits the highest Young's modulus, 159 MPa, indicating that it is the stiffest and most resistant to initial deformation under load.

In summary, these results show that both the original film thickness (comparing 190 μm with CBG-H and CBG-V) and, crucially, the heat-sealing orientation (horizontal versus vertical) have a determining impact on the mechanical profile of the chañar tar gum films. The 190 μm film is less extensible but has intermediate strength. Horizontal heat sealing (CBG-H) results in a more flexible material (higher elongation, lower modulus) but less resistant to breakage (lower tension). Surprisingly, the vertically heat-sealed sample (CBG-V) appears to optimize properties, combining

 doi:10.20944/preprints202506.1402.v1

high stretchability (elongation comparable to CBG-H) with the highest break strength and highest stiffness. This positions it as the option with the most robust and balanced mechanical profile among the samples analyzed, suggesting that vertical heat sealing is an effective process for obtaining CBG films with improved performance for applications requiring strength, stiffness, and a certain degree of flexibility. Similar details can be found in reference [25,57].

Heat Sealing Capacity

Since the ultimate goal of films developed from chañar brea gum (CBG) lies in their potential application as packaging materials, evaluating their heat-sealing capabilities becomes a critical and indispensable aspect. Heat sealing is the fundamental mechanism for creating hermetic seals and ensuring package integrity, and its quality directly determines the protection the package offers to the product it contains [58].

In this context, the mechanical behavior of CBG films subjected to heat sealing was analyzed, specifically evaluating the strength and failure mode of the seal. During tensile tests applied to the sealed samples, it was consistently observed that the predominant failure mode was not the separation or opening of the heat-sealed area, but rather fracture due to tearing of the film material adjacent to the seal line. This finding is of utmost importance, as it highlights the inherent strength of the heat seal compared to the mechanical strength of the unsealed film itself in that region. The fact that the film yields before the seal indicates that the bond formed by the heat seal is more resistant to the applied forces than the film itself, which is a key criterion for a high-quality seal in packaging applications [58].

In this work, from the tensile tests the seal strength values are CBG-H 656N/m, CBG-V 950N/m. Similar results were obtained with potato starch films con halloysite nanoclay, hadgood heat sealability and the seal strength of near 500 N/m which iscomparable with that of synthetic films (>600 N/m) [57]. Other results similar are whey protein isolate/lipid emulsion edible films [59] and used of starch films filled with nanoparticles [60].

Considering that the functionality and reliability of a package crucially depend on the integrity of its closure, the goal is to achieve a "good seal." An optimal seal is achieved at the microscopic and molecular level: it implies that, under the controlled action of heat and pressure, the interfaces between the individual layers of the film being joined effectively disappear. This occurs thanks to sufficient molecular interaction between the polymer chains of both surfaces, promoting their interdiffusion and the formation of a new, homogeneous, continuous layer in the bonded area. This molecular fusion results in an internal cohesion in the sealed region that is, ideally, as strong as or stronger than that of the base material. The evidence observed in the mechanical analysis, where the film failed before the seal, suggests that the heat-sealing process applied to CBG films achieved precisely this successful fusion, resulting in a seal with a strength superior to that of the base material, thus fulfilling a fundamental requirement for its potential use as packaging [61,62].

Heat sealing is another critical factor, along with the barrier and mechanical properties of the material developed as food packaging. A good seal must be strong enough to keep the product in the package, and airtight enough to keep the product fresh throughout its shelf life, such as cellulose films [63], wheat gluten [64], fish gelatin/ZnO nanorods [65], potato starch/halloysite nanoclay [57 Sadegh-Hassani], pullulan (PUL)/soluble soybean polysaccharide [66], Tara pod extract/soy protein isolate [15], tapioca and potato starch [67].

The heat-sealing properties of self-supporting edible films based on corn starch and a functional polysaccharide (amylose, methylcellulose, or hydroxypropylmethylcellulose) were evaluated. The highest sealing strength was obtained at 166 °C, reaching values of 0.396 N/mm for the film containing amylose, 0.211 N/mm for the film containing methylcellulose, and 0.385 N/mm for the film containing hydroxypropylmethylcellulose [1].

In reference [10], the importance of adequate sealing strength for the integrity of soluble soy polysaccharide packaging with gelatin is emphasized. Comparative results showed that the pure soluble soy polysaccharide film had a significantly lower strength (50 N/m) than the pure gelatin film

 doi:10.20944/preprints202506.1402.v1

(590 N/m). The incorporation of gelatin in blends with soluble soy polysaccharide significantly increased the sealing strength (up to 640 N/m with 60% gelatin), which is attributed to the differences in composition and structure of the materials.

Biodegradable films were prepared incorporating Tara pod extract (TPE) using soy protein isolate (SPI) as the polymer matrix. The TPE-SPI composite films showed improved mechanical properties, UV blocking, good heat sealing performance, and barrier properties [15].

In according to reference [67], developed biodegradable edible films from tapioca (T) and potato (P) starch in various proportions, heat sealing is analyzed, it presented the lowest tensile strength and greatest elongation.

A paper [11] evaluated the characterization of cellulose acetate-CNF composite films and showed that the tensile strength decreased with increasing nanofiber concentration.

According to reference [12], the pure starch film showed low strength (0.06 N/mm), possibly due to its low polymer concentration. The combined addition of 75% starch and 25% chitosan resulted in the highest strength (0.17 N/mm), suggesting that chitosan at this ratio acts as a plasticizer, enhancing molecular interdiffusion during sealing through hydrogen bonding. However, increasing the chitosan ratio decreased the strength due to its lack of thermoplasticity. The incorporation of reduced graphene oxide reduced the strength to less than 0.04 N/mm, making sealing more difficult by restricting the mobility of the polymer chains and affecting hydrogen bonding. The common failure mode was peeling, indicative of sealing below the melting point of the polymers.

3.9. Biodegradability

The biodegradability of films made from polysaccharides is one of their most notable properties and one of the main reasons for their growing interest as an alternative to conventional plastics. Polysaccharides are widely available, renewable, and, crucially, susceptible to degradation by the action of microorganisms present in various environments [68].

The biodegradation process of polysaccharide films involves the breakdown of polymer chains into simpler compounds, such as carbon dioxide, water, methane (under anaerobic conditions), and biomass, through enzymatic mechanisms carried out by bacteria, fungi, and other microbial communities. These enzymes, such as amylases (for starch), cellulases (for cellulose), and chitinases (for chitin/chitosan), hydrolyze the glycosidic bonds that link the monomeric sugar units in the polysaccharide [69].

In general, polysaccharide films offer a sustainable alternative to petroleum-derived plastics due to their ability to be reincorporated into the natural cycle through biodegradation, contributing to the reduction of plastic waste accumulation in the environment. However, it is important to consider that the speed and extent of biodegradation can vary significantly depending on the specific film formulation and the conditions of the disposal environment [66,68].

Several factors influence the speed and degree of biodegradation of a polysaccharide film, as described below. 1- Polysaccharide Type: The chemical structure and complexity of the base polysaccharide affect its susceptibility to enzymatic degradation. Polysaccharides such as starch tend to degrade more rapidly than crystalline cellulose, for example. 2- Film Structure and Composition: The crystallinity of the polymer, its molecular weight, and the presence of chain branches influence the accessibility of enzymes to degradable bonds. 3- Additives and Plasticizers: The addition of plasticizers (such as glycerol) to improve flexibility can, in some cases, increase the rate of biodegradation by facilitating water absorption and microbial activity. However, other additives may have the opposite effect. 4- Environmental Conditions: Factors such as temperature, humidity, pH, oxygen availability, and the activity of microbial populations in the environment (soil, compost, water) are crucial in determining the rate of degradation. Warm, humid environments with rich microbial activity generally accelerate the process. 5- Film Thickness: Thinner films tend to degrade faster due to a greater contact surface area available for microorganisms and enzymes [66,68,70].

Common polysaccharides used in the production of biodegradable films include:

 doi:10.20944/preprints202506.1402.v1

-Starch: Widely studied and used due to its low cost and availability. Thermoplastic starch films are biodegradable in a variety of environments [70].

-Cellulose and derivatives: Cellulose, being the most abundant natural polymer, is an important base for biodegradable films. Its derivatives, such as carboxymethylcellulose or cellophane (regenerated cellulose), are also biodegradable [71].

-Chitin and Chitosan: Obtained mainly from crustacean exoskeletons, they are polysaccharides with interesting properties for films, including their biodegradability in the presence of chitinases [72].

In this work, CBG, CBG-H and CBG-V films are completely degraded after 4 days and, for example, similar studies of materials biodegradability are: heat-sealed arabinogalactan (AG) and poly (vinyl alcohol) (PVA) films with and without vinyllin [73], heat-sealed cellulose/zein films [71], films of oxidized sucrose (starch), chitosan, calcium chloride (alginate) and blends (starch/chitosan and starch/alginate, respectively) [74], edible films based on corn starch [70] and a functional polysaccharide, such as amylose, methylcellulose or hydroxypropylmethylcellulose (HPMC) [1], FucoPol films [75], chia mucilago films [76], Chañar films [44], Lithraea molleoides gum films [33], Pachycymbiola brasiliana gum films [42], alcayota gum films [41], Tragacanth films [45], Tara gum films [77], pectins films [43,78], etc.

4. Conclusions

This study demonstrates that films developed from chañar gum (CBG), prepared by the 10% glycerin casting method and heat-sealed at 140°C, possess promising characteristics for biodegradable packaging applications. A thorough evaluation of their fundamental properties revealed crucial intrinsic relationships that dictate their heat-sealability.

Remarkable thermal stability of CBG was observed up to 200°C, with a melting point of 152.48°C, which is compatible with the sealing temperatures used. The homogeneous and nearly gapless microstructure of the heat seal, evidenced by SEM images, along with similar interchain spacing between CBG and CBG-H (4.88 nm vs. 4.66 nm), suggests good surface integration during sealing. Barrier properties improved significantly, with water vapor permeability (WVP) decreasing from 1.7 to 0.37 for CBG and CBG-H, respectively, indicating greater protection of the packaged product. Although Young's modulus decreased from 132 MPa to 96.5 MPa with the addition of glycerin (CBG-H), heat sealability reached 656 N/m, representing a robust sealing force. Furthermore, biodegradability in just 4 days highlights the potential of these films as a sustainable packaging alternative.

In summary, the integration of molecular, thermal, mechanical, and barrier properties has provided insight into how these fundamental characteristics interconnect to control the heat-sealability of chañar brea gum films. This comprehensive approach is vital to optimizing the sealing process and advancing the design of efficient and functional biodegradable packaging.

Author Contributions: Conceptualization, M.F.T. and M.M.; methodology, G.M., F.B. and M.F.T.; validation, M.F.T. and G.M.; formal analysis, M.F.T., M.F. and M.M.; investigation, M.F. and F.B.; resources, M.M.; writing—original draft preparation, M.F.T. and M.M.; writing—review and editing, M.F.T., M.F. and M.M. All authors have read and agreed to the published version of the manuscript.

Funding: PICT-2020-SERIEA-00895 (RAICES). Title: "Obtención de Polisacáridos a partir de Vegetales y Microorganismos de la Región del Semiárido de San Luis. Aplicaciones: Alimentarias, Geles y Bioempaque", 2. PROICO 2-3423, UNSL: "Bioprospección de Recursos Autóctonos Vegetales y Microbianos de la Provincia de San Luis con Potencial Uso Biotecnológico", and 3. PIP 2021/2023, IF-2021-85081432-APN-DCP#CONICET, "Valorización biotecnológica de efluentes de destilería para la obtención de productos microbianos". Institutional Research Program (UNSL): Desarrollo sostenible de productos alimenticios empleando un recurso regional como la goma brea, (2021-2022) (Res. CS 236/21).

 doi:10.20944/preprints202506.1402.v1

Data Availability Statement: The original contributions presented in the study are included in the article; further inquiries can be directed to the corresponding authors.

Acknowledgments: The authors thank the following institutions in Argentina: Instituto de Física Aplicada (INFAP-UNSL-CONICET) and Laboratorio de Investigación y Servicios de Química Física (LISeQF-UNSL). The authors also thank Javier Rigau from the Instituto de Investigación en Tecnología Química (INTEQUI-UNSL-CONICET) for their determinations of the FTIR, TGA, and DSC, and Ariel Ochoa from the Laboratorio de Membranas y Biomateriales del INFAP-CONICET-UNSL for their contributions to the mechanical test and water vapor permeability results.

Conflicts of Interest: The authors declare no conflicts of interest.

References

1. Das, M., & Chowdhury, T. (2016). Heat sealing property of starch based self-supporting edible films. *Food Packaging and Shelf Life*, 9, 64-68.
2. Khodaei, D., Álvarez, C., & Mullen, A. M. (2021). Biodegradable packaging materials from animal processing co-products and wastes: An overview. *Polymers*, 13(15), 2561.
3. Jeevahan, J. J., Chandrasekaran, M., Venkatesan, S. P., Sriram, V., Joseph, G. B., Mageshwaran, G., & Durairaj, R. B. (2020). Scaling up difficulties and commercial aspects of edible films for food packaging: A review. *Trends in Food Science & Technology*, 100, 210-222.
4. Dag, D., Jung, J., & Zhao, Y. (2023). Development and characterization of cinnamon essential oil incorporated active, printable and heat sealable cellulose nanofiber reinforced hydroxypropyl methylcellulose films. *Food Packaging and Shelf Life*, 39, 101153.
5. Yi, C., Yuan, T., Xiao, H., Ren, H., & Zhai, H. (2023). Hydrophobic-modified cellulose nanofibrils (CNFs)/chitosan/zein coating for enhancing multi-barrier properties of heat-sealable food packaging materials. *Colloids and Surfaces A: Physicochemical and Engineering Aspects*, 666, 131245.
6. Rajeshkumar, L., Ramesh, M., Bhuvaneswari, V., Balaji, D., & Deepa, C. (2023). Synthesis and thermomechanical properties of bioplastics and biocomposites: a systematic review. *Journal of Materials Chemistry B*, 11(15), 3307-3337.
7. Kalina, S., Kapilan, R., Wickramasinghe, I., & Navaratne, S. B. (2024). Potential use of plant leaves and sheath as food packaging materials in tackling plastic pollution: A Review. *Ceylon Journal of Science*, 53(1).
8. Zink, J., Wyrobnik, T., Prinz, T., & Schmid, M. (2016). Physical, chemical and biochemical modifications of protein-based films and coatings: An extensive review. *International journal of molecular sciences*, 17(9), 1376.
9. Song, X., Zuo, G., & Chen, F. (2018). Effect of essential oil and surfactant on the physical and antimicrobial properties of corn and wheat starch films. *International journal of biological macromolecules*, 107, 1302-1309.
10. Liu, C., Huang, J., Zheng, X., Liu, S., Lu, K., Tang, K., & Liu, J. (2020). Heat sealable soluble soybean polysaccharide/gelatin blend edible films for food packaging applications. *Food Packaging and Shelf Life*, 24, 100485.
11. Hazarika, K. K., Konwar, A., Borah, A., Saikia, A., Barman, P., & Hazarika, S. (2023). Cellulose nanofiber mediated natural dye based biodegradable bag with freshness indicator for packaging of meat and fish. *Carbohydrate Polymers*, 300, 120241.
12. Alves, Z., Ferreira, N. M., Ferreira, P., & Nunes, C. (2022). Design of heat sealable starch-chitosan bioplastics reinforced with reduced graphene oxide for active food packaging. *Carbohydrate Polymers*, 291, 119517.
13. Lim, W. S., Ock, S. Y., Park, G. D., Lee, I. W., Lee, M. H., & Park, H. J. (2020). Heat-sealing property of cassava starch film plasticized with glycerol and sorbitol. *Food Packaging and Shelf Life*, 26, 100556.
14. Bamps, B., Buntinx, M., & Peeters, R. (2023). Seal materials in flexible plastic food packaging: A review. *Packaging Technology and Science*, 36(7), 507-532.
15. Ren, Z., Ning, Y., Xu, J., Cheng, X., & Wang, L. (2024). Eco-friendly fabricating Tara pod extract-soy protein isolate film with antioxidant and heat-sealing properties for packaging beef tallow. *Food Hydrocolloids*, 153, 110041.

 doi:10.20944/preprints202506.1402.v1

16. Garavito, J., Peña-Venegas, C. P., & Castellanos, D. A. (2024). Production of Starch-Based Flexible Food Packaging in Developing Countries: Analysis of the Processes, Challenges, and Requirements. *Foods*, 13(24), 4096.
17. Trianti, M., Mastora, A., Nikolaidou, E., Zorba, D., Rozou, A., Giannou, V., ... & Papadakis, S. E. (2024). Development and characterization of "Greek Salad" edible films. *Food Packaging and Shelf Life*, 46, 101378.
18. Wang, R., Chen, Z., Shu, Y., Wang, Y., Wang, W., Zhu, H., ... & Ma, Q. (2024). Apple pectin-based active films to preserve oil: Effects of naturally branched phytoglycogen-curcumin host. *International Journal of Biological Macromolecules*, 266, 131218.
19. Zehra, A., Amin, T., Wani, S. M., Sidiq, H., Bashir, I., Mustafa, S., ... & Showkat, S. (2024). Chitosan-Based Films. In Polysaccharide Based Films for Food Packaging: Fundamentals, Properties and Applications (pp. 121-144). Singapore: Springer Nature, Singapore.
20. Rahman, S., Konwar, A., Gurumayam, S., Borah, J. C., & Chowdhury, D. (2025). Sodium Alginate-chitosan-starch based glue formulation for sealing biopolymer films. *Next Materials*, 7, 100507.
21. Uribarrena, M., Cabezudo, S., Núñez, R. N., Copello, G. J., de la Caba, K., & Guerrero, P. (2025). Development of smart films based on soy protein and cow horn dissolved in a deep eutectic solvent: Physicochemical and environmental assessment. *International Journal of Biological Macromolecules*, 291, 139045.
22. Nafchi, A. M., Nassiri, R., Sheibani, S., Ariffin, F., & Karim, A. A. (2013). Preparation and characterization of bionanocomposite films filled with nanorod-rich zinc oxide. *Carbohydrate Polymers*, 96(1), 233-239.
23. Ortega, Florencia. (2021). Tesis Doctoral. Materiales biodegradables con nanopartículas de plata con capacidad antimicrobiana para mejorar los procesos de conservación de alimentos. Universidad Nacional de la Plata, La Plata, Argentina.
24. Bertuzzi, M. A., Slavutsky, A. M., & Armada, M. (2012). Physicochemical characterisation of the hydrocolloid from Brea tree (Cercidium praecox). *International Journal of Food Science & Technology*, 47(4), 768-775.
25. Bertuzzi, M. A., & Slavutsky, A. M. (2013). Formulation and Characterization of Film Based on Gum Exudates from Brea Tree (Cercidium praecox). *Journal of Food Science and Engineering*, 3 113-122.
26. Slavutsky, A. M., Bertuzzi, M. A., Armada, M., García, M. G., & Ochoa, N. A. (2014). Preparation and characterization of montmorillonite/brea gum nanocomposites films. *Food Hydrocolloids*, 35, 270-278.
27. Slavutsky, A. M., & Bertuzzi, M. A. (2015). Thermodynamic study of water sorption and water barrier properties of nanocomposite films based on brea gum. *Applied Clay Science*, 108, 144-148.
28. Cecchini, J. P., Spotti, M. J., Piagentini, A. M., Milt, V. G., & Carrara, C. R. (2017). Development of edible films obtained from submicron emulsions based on whey protein concentrate, oil/beeswax and brea gum. *Food Science and Technology International*, 23(4), 371-381.
29. Slavutsky, A. M., Gamboni, J. E., & Bertuzzi, M. A. (2018). Formulation and characterization of bilayer films based on Brea gum and Pectin. *Brazilian Journal of Food Technology*, 21, e2017213.
30. Masuelli, M. A., Slatvustky, A., Ochoa, A., & Bertuzzi, M. A. (2018). Physicochemical Parameters for Brea Gum Exudate from Cercidium praecox Tree. *Colloids and Interfaces*, 2(4), 72.
31. Torres, M. F., Lazo Delgado, L., Filippa, M., Masuelli, M. A. (2020). Effect of Temperature on Mark-Houwink-Kuhn-Sakurada (MHKS) Parameters of Chañar Brea Gum Solutions. *Journal of Polymer and Biopolymer Physics Chemistry*, 8(1), 28-30.
32. Torres, M. F., Lazo Delgado, L., D'Amelia, R., Filippa, M., Masuelli, M. (2021). Sol/gel transition temperature of chañar brea gum. *Current Trends in Polymer Science*, 20, 83-93.
33. Becerra, F., Garro, M. F., Melo, G., & Masuelli, M. (2024). Preparation and Characterization of Lithraea molleoides Gum Flour and Its Blend Films. *Processes*, 12(11), 2506.
34. Rulli, M.M.; Villegas, L.B.; Barcia, C.S.; Colin, V.L. Bioconversion of sugarcane vinasse into fungal biomass protein and its potential use in fish farming. J. Environ. Chem. Eng. 2021, 9, 106136.
35. Deng, C.; Hu, Z.; Fu, H.; Hu, M.; Xu, X.; Chen, J. Chemical analysis and antioxidant activity in vitro of β-D-glucan isolated from Dictyophora indusiate. *Int. J. Biol. Macromol.*, 2012, 51, 70-75.
36. Kaur, R.; Arora, S.; Singh, B. Antioxidant activity of the phenol rich fractions of leaves of Chukrasia tabularis A. Juss. *Bioresour. Technol.*, 2008, 99, 7692-7698.

 doi:10.20944/preprints202506.1402.v1

37. Ainsworth, E.A.; Gillespie, K.M. Estimation of total phenolic content and other oxidation substrates in plant tissues using Folin-Ciocalteu reagent. *Nat. Protoc.*, 2007, 2, 875-877.
38. Zanon, M.; Masuelli, M. Purification and characterization of alcayota gum. *Biopolym. Res.*, 2018, 2, 105.
39. Al Sagheer, F.A.; Al-Sughayer, M.A.; Muslim, S.; Elsabee, M.Z. Extraction and characterization of chitin and chitosan from marine sources in Arabian Gulf. *Carbohydr. Polym.*, 2009, 77, 410-419.
40. Barbosa, H.F.; Francisco, D.S.; Ferreira, A.P.; Cavalheiro, É.T. A new look towards the thermal decomposition of chitins and chitosans with different degrees of deacetylation by coupled TG-FTIR. *Carbohydr. Polym.*, 2019, 225, 115232.
41. Zanon, M.; Masuelli, M.A. Alcayota gum films: Experimental reviews. *J. Mater. Sci. Chem. Eng.*, 2018, 6, 11-58.
42. Masuelli, M. A., Lazo, L., Becerra, F., Torres, F., Illanes, C. O., Takara, A., Auad, M. L., Bercea, M. (2024). Physical and Chemical Properties of Pachycymbiola brasiliana Eggshells-From Application to Separative Processes. *Processes*, 12(4), 814.
43. Ruano, P., Delgado, L. L., Picco, S., Villegas, L., Tonelli, F., Merlo, M. E. A., ... & Masuelli, M. (2019). Extraction and Characterization of Pectins from Peels of Criolla Oranges (Citrus sinensis): Experimental Reviews. In Pectins-Extraction, Purification, Characterization and Applications. Martin Masuelli Ed. IntechOpen, London, UK.
44. Lazo, L.; Melo, G.M.; Auad, M.L.; Filippa, M.; Masuelli, M.A. Synthesis and characterization of Chañar gum films. *Colloids Interfaces*, 2022, 6, 10.
45. Illanes, C.O.; Takara, E.A.; Masuelli, M.A.; Ochoa, N.A. pH-responsive gum tragacanth hydrogels for high methylene blue adsorption. *J. Chem. Technol. Biotechnol.*, 2024, 99, 31-39.
46. Adhikary, N. D., Bains, A., Sridhar, K., Kaushik, R., Chawla, P., & Sharma, M. (2023). Recent advances in plant-based polysaccharide ternary complexes for biodegradable packaging. *International Journal of Biological Macromolecules*, 253, 126725.
47. Acosta-Ferreira, S.; Castillo, O.S.; Madera-Santana, J.T.; Mendoza-García, D.A.; Núñez-Colín, C.A.; Grijalva-Verdugo, C.; Villa-Lerma, A.G.; Morales-Vargas, A.T.; Rodríguez-Núñez, J.R. Production and physicochemical characterization of chitosan for the harvesting of wild microalgae consortia. *Biotechnol. Rep.*, 2020, 28, e00554.
48. 48. 47. Chel-Guerrero, L.; Betancur-Ancona, D.; Aguilar-Vega, M.; Rodríguez-Canto, W. Films properties of QPM corn starch with Delonix regia seed galactomannan as an edible coating material. *Int. J. Biol. Macromol.*, 2024, 255, 128408.
49. Yazdi, M. K., Seidi, F., Jin, Y., Zarrintaj, P., Xiao, H., Esmaeili, A., ... & Saeb, M. R. (2021). Crystallization of polysaccharides. Polysaccharides: Properties and Applications, 283-300.
50. Luo, A., Hu, B., Feng, J., Lv, J., & Xie, S. (2021). Preparation, and physicochemical and biological evaluation of chitosan Arthrospira platensis polysaccharide active films for food packaging. *Journal of Food Science*, 86(3), 987-995.
51. Nahas, E. O., Furtado, G. F., Lopes, M. S., & Silva, E. K. (2025). From Emulsions to Films: The Role of Polysaccharide Matrices in Essential Oil Retention Within Active Packaging Films. *Foods*, 14(9), 1501.
52. Du, B., Jeepipalli, S. P., & Xu, B. (2022). Critical review on alterations in physiochemical properties and molecular structure of natural polysaccharides upon ultrasonication. *Ultrasonics Sonochemistry*, 90, 106170.
53. Demircan, B., McClements, D. J., & Velioglu, Y. S. (2025). Next-Generation Edible Packaging: Development of Water-Soluble, Oil-Resistant, and Antioxidant-Loaded Pouches for Use in Noodle Sauces. *Foods*, 14(6), 1061.
54. Bumbudsanpharoke, N., Harnkarnsujarit, N., Chongcharoenyanon, B., Kwon, S., & Ko, S. (2023). Enhanced properties of PBAT/TPS biopolymer blend with CuO nanoparticles for promising active packaging. *Food Packaging and Shelf Life*, 37, 101072.
55. Dong, Y., Rao, Z., Liu, Y., Zheng, X., Tang, K., & Liu, J. (2023). Soluble soybean polysaccharide/gelatin active edible films incorporated with curcumin for oil packaging. *Food Packaging and Shelf Life*, 35, 101039.
56. Bhat, R., Abdullah, N., Din, R. H., & Tay, G. S. (2013). Producing novel sago starch based food packaging films by incorporating lignin isolated from oil palm black liquor waste. *Journal of Food Engineering*, 119(4), 707-713.

 doi:10.20944/preprints202506.1402.v1

57. Sadegh-Hassani, F., & Nafchi, A. M. (2014). Preparation and characterization of bionanocomposite films based on potato starch/halloysite nanoclay. *International journal of biological macromolecules*, 67, 458-462.
58. Chhikara, S., & Kumar, D. (2022). Edible coating and edible film as food packaging material: A review. *Journal of Packaging Technology and Research*, 6(1), 1-10.
59. Kim, S. J., & Ustunol, Z. (2001). Thermal properties, heat sealability and seal attributes of whey protein isolate/lipid emulsion edible films. *Journal of food science*, 66(7), 985-990.
60. Nafchi, A. M. (2013). Mechanical, barrier, physicochemical, and heat seal properties of starch films filled with nanoparticles. *Journal of Nano Research*, 25, 90-100.
61. Shah, Y. A., Bhatia, S., Al-Harrasi, A., Oz, F., Khan, M. H., Roy, S., ... & Pratap-Singh, A. (2024). Thermal properties of biopolymer films: Insights for sustainable food packaging applications. *Food Engineering Reviews*, 16(4), 497-512.
62. Demircan, B., & Velioglu, Y. S. (2025). Revolutionizing single-use food packaging: a comprehensive review of heat-sealable, water-soluble, and edible pouches, sachets, bags, or packets. *Critical reviews in food science and nutrition*, 65(8), 1497-1517.
63. Chu, Y. (2023). Regenerated Cellulose Films with Heat Sealability and Improved Barrier Properties for Sustainable Food Packaging. McGill University, Montreal, Canada.
64. Cho, S. W., Ullsten, H., Gällstedt, M., & Hedenqvist, M. S. (2007). Heat-sealing properties of compression-molded wheat gluten films. *Journal of Biobased Materials and Bioenergy*, 1(1), 56-63.
65. Rouhi, J., Mahmud, S., Naderi, N., Ooi, C. R., & Mahmood, M. R. (2013). Physical properties of fish gelatin-based bio-nanocomposite films incorporated with ZnO nanorods. *Nanoscale research letters*, 8, 1-6.
66. Zhao, F., Jiang, L., Wang, C., Li, S., Sun, D., Ma, Q., ... & Jiang, W. (2024). Flexibility, dissolvability, heat-sealability, and applicability improvement of pullulan-based composite edible films by blending with soluble soybean polysaccharide. *Industrial Crops and Products*, 215, 118693.
67. Roidoung, S., Sonyiam, S., & Fugthong, S. (2025). Development of heat sealable film from tapioca and potato starch for application in edible packaging. *Journal of Food Science and Technology*, 62(2), 389-395.
68. Aleksanyan, K. V. (2023). Polysaccharides for biodegradable packaging materials: Past, present, and future (Brief Review). *Polymers*, 15: 451.
69. Zhao, Y., Li, B., Li, C., Xu, Y., Luo, Y., Liang, D., & Huang, C. (2021). Comprehensive review of polysaccharide-based materials in edible packaging: A sustainable approach. *Foods*, 10(8), 1845.
70. López, O. V., Lecot, C. J., Zaritzky, N. E., & García, M. A. (2011). Biodegradable packages development from starch based heat sealable films. *Journal of Food Engineering*, 105(2), 254-263.
71. Chu, Y., Popovich, C., & Wang, Y. (2023). Heat sealable regenerated cellulose films enabled by zein coating for sustainable food packaging. *Composites Part C: Open Access*, 12, 100390.
72. Jongjun, Y., Pornprasert, P., & Prateepchanachai, S. (2024). Improvement of heat-sealing strength of chitosan-based composite films and product costs analysis in the production process. *Journal of Applied Research on Science and Technology*, 23(1), 251817-251817.
73. Zhang, H., Li, M., Liu, Z., Li, R. A., & Cao, Y. (2024). Heat-sealable, transparent, and degradable arabinogalactan/polyvinyl alcohol films with UV-shielding, antibacterial, and antioxidant properties. *International Journal of Biological Macromolecules*, 275, 133535.
74. Janik, W., Nowotarski, M., Shyntum, D. Y., Bana?, A., Krukiewicz, K., Kud?a, S., & Dudek, G. (2022). Antibacterial and biodegradable polysaccharide-based films for food packaging applications: Comparative study. *Materials*, 15(9), 3236.
75. Ferreira, A. R., Torres, C. A., Freitas, F., Reis, M. A., Alves, V. D., & Coelhoso, I. M. (2014). Biodegradable films produced from the bacterial polysaccharide FucoPol. *International Journal of Biological Macromolecules*, 71, 111-116.
76. Fernandes, S. S., Romani, V. P., da Silva Filipini, G., & G Martins, V. (2020). Chia seeds to develop new biodegradable polymers for food packaging: Properties and biodegradability. *Polymer Engineering & Science*, 60(9), 2214-2223.
77. Masuelli, M. A. & García, M. G. (2017). Biopackaging: Tara Gum Films. In Advances in Physicochemical Properties of Biopolymers. Part 2, pp. 876-898. Martin Masuelli & Denis Renard Eds. Bentham Publishing. Dubai, UEA.

 doi:10.20944/preprints202506.1402.v1

78. García, María Guadalupe, Masuelli, Martin A. (2022). Effect of Cross-Linking Agent on Mechanical and Permeation Properties of Criolla Orange Pectin". In Pectin-The New-Old Polysaccharides, Martin Masuelli Ed. INTECH, Rijeka, Croatia.